Special Conference Edition, April, 2022
http://dx.doi.org/10.4314/bajopas.v13i1.26S

Bayero Journal of Pure and Applied Sciences, 13(1): 149 - 162
ISSN 2006 – 6996

CORROSION INHIBITION OF ZINC IN 0.5 M HNO_3 USING *Azadirachta indica* EXTRACT: EXPERIMENTAL AND COMPUTATIONAL STUDY

Saifullahi Lawal Muhammad and Muhammad Bashir Ibrahim
Department of Chemistry, Federal University, Gashua, Yobe, Nigeria.
Department of Pure and Industrial Chemistry, Bayero University, Kano, Nigeria.
Corresponding authors email: Saifullahi Lawal Muhammad
Address: Department of Chemistry, Federal University, Gashua, Yobe, Nigeria.
Email: mlawalfagge@gmail.com:Phone: +2348101221686

ABSTRACT
Azadirachta indica (AI) leave extract was investigated as a zinc corrosion inhibitor in nitric acid solution using experimental weight loss measurements and computational studies. Inhibition efficiency and corrosion rate was studied using effect of immersion time (1 – 4 h), effect of temperature (30 – 60 ℃) and inhibitor concentration (0.20 – 0.80 g/L). Corrosion rate increases with increase in temperature and decrease with increased in immersion time. Inhibition efficiency of the extract increases with increased in inhibitor concentration reaching 53.09% at 4 hours immersion time. Adsorption isotherm studies show that the experimental data was best fit into Freundlich isotherm ($R^2 = 0.9986 - 0.9995$). and the adsorption mechanism can be described as physisorption (-5.75 to -9.48 kJmol^{-1}). The adsorption process indicated feasible and spontaneous process from the large negative values of ΔG_{ads}. The values of enthalpy are all positive indicating endothermic process of adsorption. Activation energy was found to increase with increase in inhibitor concentration which increase the energy barrier of the corrosion reaction. Computational studies were carried out using density functional theory (DFT) and molecular dynamic simulation (MDS) and the result revealed that ADE has strong interaction with Zn (1 1 0) surface than AME and ADME as such it has higher adsorption energy (39.29, 11.32 and 10.02 kcal/mol) and inhibition efficiency. The experimental inhibition efficiency can be correlated to the adsorption of such molecules of inhibitor on metal surface that facilitate in reducing the corrosion of zinc in nitric acid solution. Hence, AI extract was found to be good inhibitor for the corrosion of zinc in nitric acid medium.
Keywords: Zinc, corrosion, inhibitor, azadirachta indica (AI) leave extract, density functional theory (DFT), molecular dynamic simulation (MDS).

INTRODUCTION

Zinc is a metal with numerous industrial applications due to it is cost effectiveness and is mainly used for the corrosion protection of steel. Zinc is an industrially important metal, however, it is corroded by many agents, of which aqueous acids are the most dangerous (Al-Saadi and Al-Safi, 2011).

Corrosion is the deterioration of metal by an attack from chemicals (acids, base, oil and salt) or reaction with their environment. It's a constant and continuous process, often difficult to abolish completely. Preventing the process from occurring will be more practical and achievable than complete abrogation (Srikanth and Sivakumar, 2020; Dubey, 2020). The use of aggressive medium in industrial application cannot be ignored, due to their important areas of application such as acid pickling, acid cleaning, acid rescaling and oil well cleaning (Seifzadeh *et al.,* 2008). Nitric acid is one of the most widely used corrosive media that attracted a great deal of research on metal corrosion (Madkour and Elshamy, 2016).

Among various inhibitors, organic compounds containing heteroatoms such as sulphur, oxygen, nitrogen and phosphorus, π electrons in triple or conjugated double bonds have the capacity or ability to act as good corrosion inhibitor as they can be easily adsorbed onto a metal surface. However the use of synthesized compounds containing this heteroatoms is been limited due to environmental safety and regulation.

The focus of researchers nowadays has shifted to sourcing inhibitors from available natural products. This is because such inhibitors are biodegradable, cheap, non-toxic and environmentally friendly (Sharma *et al.,* 2015; Abakedi and Asuquo, 2016; Dalhatu *et al.,* 2018). The traditional methods for evaluating the inhibition efficiency of inhibitors include weight loss measurement, polarization curves and electrochemical impedence spectroscopy, however these are time consuming and expensive (Umaru and Ayuba, 2020a). The alternative way of determining the inhibition efficiency of organic inhibitors are the use of improve computer software such as density functional theory (DFT) and molecular dynamic simulation (MDS) which are fast and powerful tools in predicting the corrosion inhibition efficiencies of inhibitor molecules (Madkour and Elshamy, 2016; Umaru and Ayuba, 2020b; Udhayakala *et al.,* 2012). Recently Quantum chemical calculations are used to determine the interaction between the inhibitor molecules and metal surface (El Hendawy *et al.,* 2021). The use of theoretical parameters allows the characterization of molecular structures of inhibitors and suggests a mechanism for their interaction with metal surface (Ogunyemi and Adejoro, 2019).

Computational parameters were calculated from the values of energy of the highest occupied molecular orbital (E_{HOMO}) and the lowest unoccupied molecular orbital (E_{LUMO}) using density functional theory (DFT) (Al-Mazaideh *et al.,* 2016; Elmsellem *et al.,* 2017). Quantum chemical calculation alone are not sufficient to study the interaction between inhibitor molecules and metal surface (Ayuba *et al.,* 2020). Therefore, there is need for experimental evaluation of adsorption mechanism between the inhibitor molecules and metal surface (Hammouti *et al.,* 2010). Molecular dynamic simulation has the capacity to provide the actual interaction and binding energy between the inhibitor molecule and metal surface (Ayuba *et al.,* 2018).

The aim of this present work is to study the inhibition potential of leave extract of *Azadirachta indica* (AI) against the corrosion of zinc in 0.5M HNO_3 solution and compare the result with computational study using quantum chemical parameters of the molecules obtained from neem tree leave. This can be achieved through quantum chemical calculations and molecular dynamic simulations.

Experimental

a. Preparation of metal couple

The zinc sheet was obtained from the market and was characterized using energy dispersed X-ray (EDX). Rectangular specimen sheets of zinc metal of thickness 0.2 cm was mechanically press and cut to form different coupons, each of their dimension was 2.0 × 2.0 cm. Each coupon was degrease by washing with ethanol then dry in acetone and preserve in desiccator. The working surface of the zinc coupons was carefully and lightly polish with SiC polishing paper in order to remove the oxide layer and prevent the reactions that would otherwise take place with the acid and zinc oxide layer (Venkata and Pankaj, 2017).

b. Plant sample collection and preparation

Fresh leave sample of neem tree (Family: Meliaceae) was obtained within the Bayero University, Kano old site premises, Nigeria. It was authenticated in the herbarium research laboratory, Bayero University, Kano (Herbarium Accession number BUKHAN 312) with the following identities: Kingdom – Plantae; Family – Meliaceae; Genus – Azadirachta; Specie – *Azadirachta indica*; Common name – Neem tree (Leave); Local name – Darbejiya. The sample was washed with water, then shred and shade dry at 30℃ for atleast seven days. Afterward, the sample was grinded into powdered form, sieved into fine powder, and stored in a plastic jar with air tight lid (Okewale and Omoruwuo, 2018).

c. Medium

The corrosive solution was prepared by diluting analytical grade of HNO_3 with distilled water to obtain the desired concentration of 0.5 M HNO_3 using serial dilution.

d. Extraction of the Plant Leave

Air dried leave 250g was weighed and grounded using mortar and pestle, followed by maceration with 1000 ml of 99% ethanol, subsequently, the solution was shaken to enable the extraction of the leave content in large glass trough with cover at room temperature. The solution was allowed to stand for at least one week with vigorously shaking each day, in order to obtain homogeneous extract (Abakedi and Asuquo, 2016). Afterward the leave was filtered repeatedly so as to have clear extract without traces of leaf particles. The filtrate was evaporated under reduced pressure using rotary vapour and then dried at 100℃ for few minute in oven to constant weight, leaving a dark green extract in a beaker. The extract obtained was stored in desiccator for further used (Tuaweri *et al.,* 2015; Vashi and Patel, 2015; Itodo *et al.,* 2018).

e. Weight loss measurements.

The prepared zinc coupons were utilized for weight loss measurements. Weight loss experiment was carried out as reported elsewhere (Vashi and Patel, 2015). The weight loss (W_L) was determined using the following relation:

$W_L = W_0 - W_f$ (1)

Where: W_0 is the zinc weight before immersion in the corrosive medium.

W_f is the zinc weight after immersion in the corrosive medium.

$C_R = \frac{weight\ loss}{area \times time \times density} \times 8.76 \times 10^4$ (2)

$where\ w$ is the corrosion weight loss of zinc (g), area of the coupon (cm^2), t (h), and density of zinc in ($g\ cm^{-3}$), Corrosion rate (C_R) in mm/year (Sharma and Peter, 2017).

The inhibition efficiency of the extract will be calculated using the following relation:

$I.E.(\%) = \frac{W_u - W_i}{W_u} \times 100$ (3)

Where: W_u is weight loss without inhibitor, W_i is weight loss with inhibitor. The surface coverage (θ) of the zinc specimen for different inhibitor concentration in HNO_3 solution were evaluated by weight loss experiments using the following (Vashi and Patel, 2015) equation:

$\theta = \frac{W_u - W_i}{W_u}$ (4)

f. Fourier Transform Infrared Spectroscopy (FT-IR) Analysis

The FT-IR analysis was carried out on neem leave, unreacted zinc, and that of the corrosion products in 0.5 M/0.8 g/L HNO_3 inhibited solution at 303 K after immersion time of 4 hours to determine the structural organization of the neem extract under study, uncorroded metal, and corrosion products (Okewale and Omoruwuo, 2018). The analysis was carried out using Agilent Technology, FT-IR (Cary 630) Fourier Transform Infrared Spectrophotometer, by scanning the sample through full scale wave number range (4000-650 cm^{-1}).

g. Scanning Electron Microscopy (SEM) Analysis

The surface examination of zinc specimen for both before and after inhibition with neem leave extract was examined with scanning electron microscopy (SEM) model (PR: X : phenonm World 800-07334), Scanned images of the unreacted, uninhibited and inhibited metal at 0.00 g/L and 0.8 g/L inhibitor concentration at 303 K in 0.5 M HNO_3 concentration were determined after 4 hours at an accelerating voltage of 15.00kV and x 500 magnification.

Computational Methods

a. Quantum Chemical Parameters

Quantum chemical calculations were excuted using density functional theory (DFT) programs in DMol3 with function B3LYP and DND as basic set as contained in the material studio 8.0 software (Accelrys, Inc.) which provide an insights into chemical reactivity and selectivity, in terms of global parameters such as electronegativity (χ), hardness (η), and softness (σ), energy of the frontier molecular orbitals (E_{HOMO} and E_{LUMO}), frontier orbitals (HOMO and LUMO), and energy gap (ΔE) were evaluated (Al-Mazaideh *et al.,* 2016; Elmsellem *et al.,* 2017; Ayuba *et al.,* 2020; Umaru and Ayuba, 2020b).

Hence, for an N-electron system with total electronic energy E and an external potential v(r), the chemical potential μ, known as the negative of the electronegativity χ, has been defined as the first derivative of E with respect to N at constant v(r) as expressed in equation (5) (Umaru and Ayuba, 2020a).

$\chi = -\mu = -\left(\frac{\partial E}{\partial N}\right) v(r)$ (5)

Hardness has been defined within DFT as the second derivative of E with respect to N at constant v(r) as expressed in equation (6) (Umaru and Ayuba, 2020a).

$\eta = \left(\frac{\partial E^2}{\partial N^2}\right) v(r) = \left(\frac{\partial u}{\partial N}\right) v(r)$ (6)

The ionization potential and electron affinity are related to the energy of highest molecular orbital (E_{HOMO}), and lowest unoccupied molecular orbital (E_{LUMO}) which are defined as in equation (7) and (8) (Elmsellem *et al.,* 2017; Ayuba *et al.,* 2020; Umaru and Ayuba, 2020a).

$I = -E_{HOMO}$ (7)

$A = -E_{LUMO}$ (8)

The absolute electronegativity (χ), and global hardness (η) of the inhibitor molecule are also related this parameters mentioned above (Al-Mazaideh *et al.,* 2016; Elmsellem *et al.,* 2017; Ayuba *et al.,* 2020; Umaru and Ayuba, 2020b).

$\chi = \frac{I+A}{2}$, $\chi = -\frac{1}{2}(E_{HOMO} + E_{LUMO})$ (9)

$\eta = \frac{I-A}{2}$, $\eta = -\frac{1}{2}(E_{HOMO} - E_{LUMO})$ (10)

Global softness can also be defined in equation (11)

$\sigma = \frac{1}{\eta}$ (11)

Also, the energy change of the back donation of the molecule is directly proportional to the hardness of the molecule, as described in equation (12) below (El Hendawy *et al.,* 2021).

$\Delta E_{back-donation} = -\frac{\eta}{4}$ (12)

The donation of an electrons from the inhibitor molecule to the Zn surface metal was calculated using the fraction of electron transferred (ΔN), in equation (13).

$\Delta N = \frac{\chi_{Zn} - \chi_{Inh}}{2(\eta_{Zn} + \eta_{Inh})}$ (13)

Where $\chi_{Zn} = 4.45eV$, and χ_{Inh} stands for absolute electronegativity of zinc and the inhibitor molecule respectively. $\eta_{Zn} = 4.94eV$, and η_{Inh} stands for absolute global hardness of zinc and the inhibitor molecule respectively (Benedetti *et al.,* 2015; Ayuba *et al.,* 2020).

b. Molecular Dynamic Simulation

Molecular Dynamic (MD) was executed using forcite quench MD simulation house in the Material Studio 8.0 software (Accelrys, Inc.) so as

to examine the interaction between the studied molecules and Zn surface. Hence, the optimized structure of the molecules and the Zn surface were utilized for simulation. This was aimed at sampling three different energy minima of the quenched dynamics in order to obtain an average global minimum (Umaru and Ayuba, 2020b; Ayuba *et al.,* 2020). Among various Zn surfaces available, the cleaved Zn (1 1 0) plane was selected and utilized due to its stability and higher densely packed atoms.

The simulation were conducted on 6 x 5 Zn (1 1 0) surface using the smart algorithm and condensed-phase optimized molecular potentials for atomistic simulation studies (COMPASS) force field. To avoid possible molecular edging effects which may occur during the docking process, the built Zn slab was significantly relatively larger than the molecule to adequately accommodate the adsorbed molecule. The temperature for the simulation was maintained at 350K, 5ps simulation time and 1 fs time step.

The optimized Zn surface was utilized for docking process. The system quench was achieved every 250 steps with the Zn (1 1 0) atoms well constrained. To determine the energy of adsorption (E_{ads}) and the binding energies (BE) of the single molecule adsorbed onto the Zn (1 1 0) surface which provides access of relating them to inhibition efficiencies, the following equation (14) is used (Ayuba *et al.,* 2020).

$$E_{ads} = -BE = E_{complex} - (E_{Zn} + E_{inhibitor}) \quad (14)$$

Where $E_{complex}$ is the total energy of the Zn surface and inhibitor, E_{Zn} is the energy of the Zn surface without the inhibitor, and $E_{inhibitor}$ is the energy of the inhibitor without the Zn surface.

The extracts component utilized for computational analyses in this study were obtained from GC-MS analysis of neem tree leave extracts which are; Acetic acid, (4-chloro-2-methyl phenoxy)-, undecyl ester (AME), Acetic acid, (4-chloro phenoxy)-, dodecyl ester (ADE), and Acetic acid, (4-chloro-3-methyl-phenoxy)-, 4,8-dimethyl-undecyl ester (ADME) and their structure are shown as Figure 1.

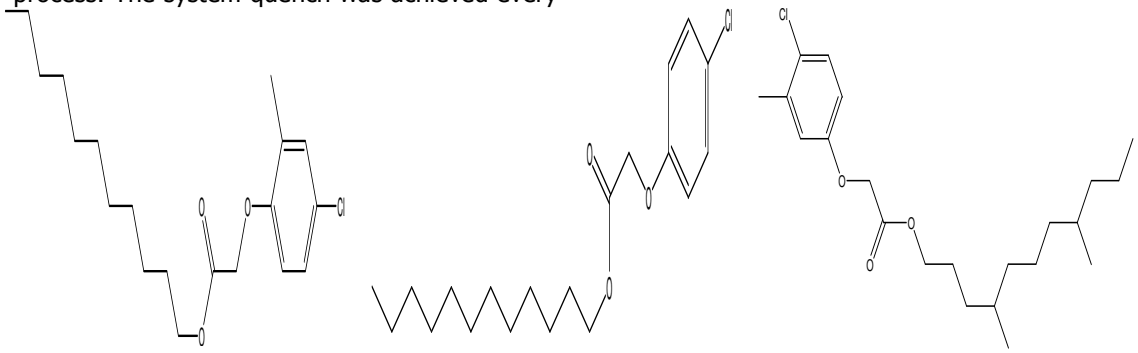

(a) (b) (c)

Figure 1: Chemical structures of the studied molecules: (a) Acetic acid, (4-chloro-2-methyl phenoxy)-, undecyl ester (AME) (b) Acetic acid, (4-chloro phenoxy)-, dodecyl ester (ADE) (c) Acetic acid, (4-chloro-3-methyl-phenoxy)-, 4,8-dimethyl-undecyl ester (ADME).

RESULTS AND DISCUSSION

Weight loss measurement

Table 1: Corrosion parameters for zinc corrosion in an aqueous solution of 0.5 M HNO_3 in absence and presence of different concentration of inhibitor from weight loss measurements.

	Temperature											
Conc.	**30**℃			**40**℃			**50**℃			**60**℃		
(g/L)	C_R mm/yr	IE %	θ	C_R mm/yr	IE %	θ	C_R mm/yr	IE %	θ	C_R mm/yr	IE %	θ
0.00	388.81	-	-	391.52	-	-	470.37	-	-	517.84	-	-
0.20	333.21	14.30	0.1430	347.61	11.22	0.1122	428.59	8.88	0.0888	485.19	6.30	0.063
0.40	295.71	23.94	0.2394	316.38	19.19	0.1919	397.08	15.58	0.1558	454.68	12.19	0.122
0.60	241.81	37.80	0.3780	280.31	28.40	0.2840	361.86	23.06	0.2306	425.74	17.78	0.178
0.80	182.36	53.09	0.5309	245.66	37.25	0.3725	330.78	29.67	0.2967	402.49	22.27	0.223

Table 2: Weight loss parameters at different contact time

Time (hour)	C_R (mm/yr)		IE (%)	θ
	Uninhibited	Inhibited		
1.00	1084.16	616.51	43.13	0.4313
2.00	614.23	323.08	47.40	0.4740
3.00	472.79	230.79	51.19	0.5119
4.00	388.81	182.36	53.09	0.5309

The weight loss experiment were conducted in 0.5 M HNO_3 acid solution in the absence and presence of various concentration plant extract ranging from 0.20 g/L to 0.80 g/L. the weight loss data was used to calculate the corrosion rate and inhibition efficiency and the values are given in Table 1. It has been observed from the Table that addition of plant extract to 0.5 M HNO_3 acid solution reduced the weight loss of zinc and decreases the corrosion rate, also inhibition efficiency increases with increase in extract concentration reaching 53.09% at 0.80 g/L inhibitor concentration for a period of 4 hours. The results also indicated that the plant extract can serve as effective corrosion inhibitor for zinc in 0.5 M HNO_3 acid solution.

Also, inhibition efficiency was found to decrease as the temperature increases as shown in Figure 5, and the decrease in inhibition efficiency with increase in temperature suggests a possible desorption of some of the adsorbed inhibitors from metal surface at higher temperature. Hence, such behaviour shows that the molecules of inhibitor were physically adsorbed on metal surface and the mechanism of adsorption can be described as physisorption (Khadraoui *et al.,* 2013; Sobhi *et al.,* 2015; Itodo *et al.,* 2018).

Corrosion rate was found to increase with rise in temperature as shown in Figure 4. Furthermore, an increase in inhibition efficiency with increase in extract concentration indicates strong interaction between the extract and metal surface (Abakedi and Asuquo, 2016).

a. Effect of immersion time

The result in Table 2 show the variation of corrosion rate and inhibition efficiency with time, and it was observed from the result that corrosion rate in both uninhibited and inhibited solution decreases with increase in immersion time while inhibition efficiency of the plant extracts increases with increase in time and this observation are in agreement with the findings (Jane and Nakara, 2019). The variation of corrosion rate with time and inhibition efficiency with time can be seen in Figure 2 and 3 respectively.

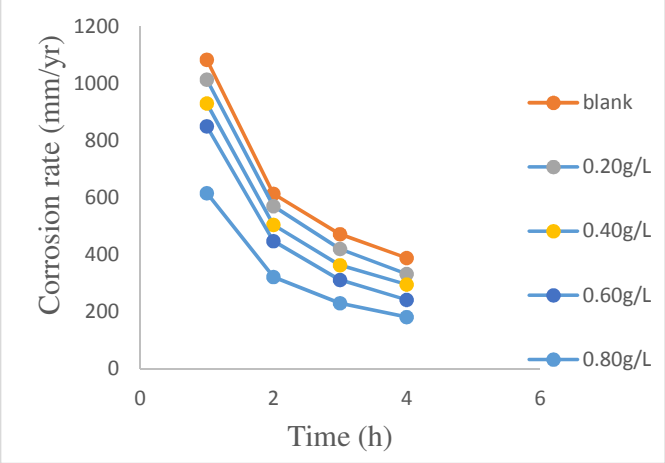

Figure 2: Variation of corrosion rate with time

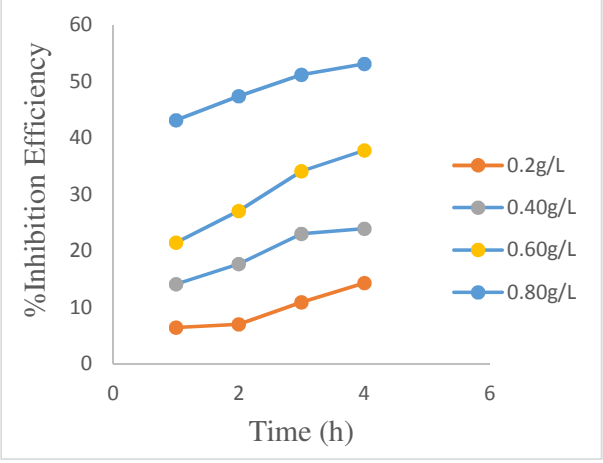

Figure 3: Variation of %Inhibition efficiency with time

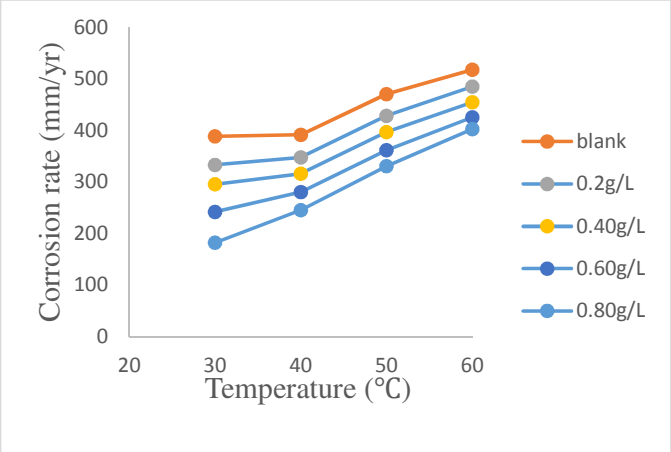

Figure 4: Variation of corrosion rate with temperature

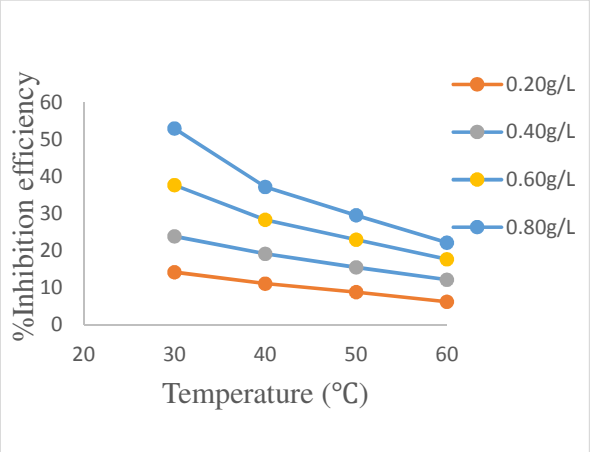

Figure 5: Variation of %Inhibition efficiency with temperature

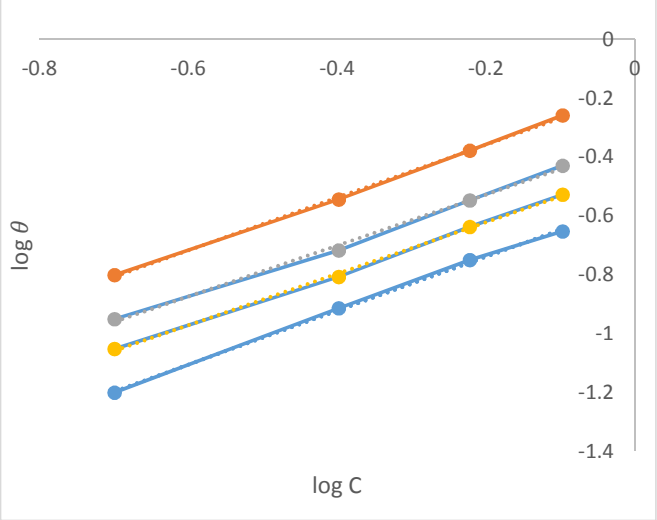

Figure 6: Freundlich Isotherm for neem leave extract at 0.5 M HNO_3 and at various Temperature

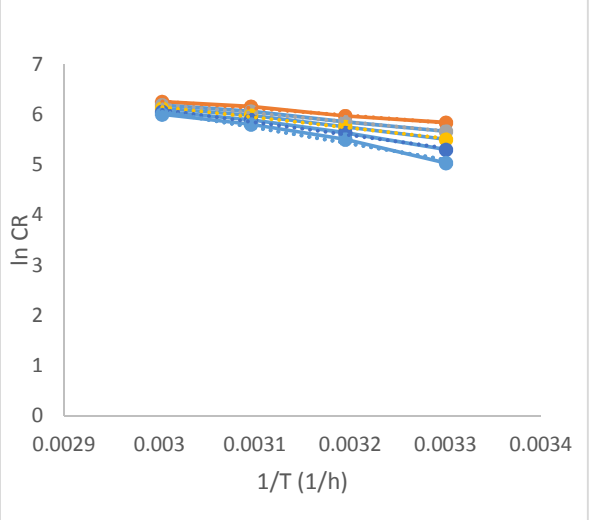

Figure 7: Arrhenius plot for 0.5 M HNO_3 and various inhibitor concentration

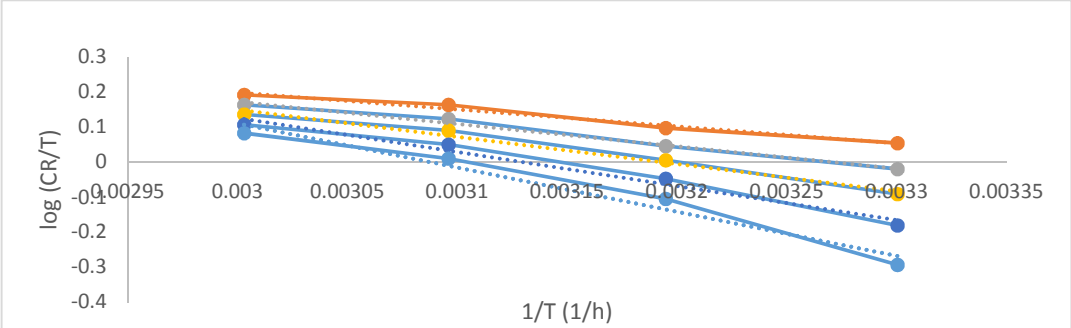

Figure 8: Plot for transition state equation at 0.5 M HNO_3

b. Fourier Transform Infrared (FT-IR) Spectroscopy

The FT-IR analysis was carried out on the neem leave extracts, unreacted zinc and that of the corrosion product in 0.5 M HNO_3 and 0.80 g/L inhibitor concentration to determine the structural organization of neem leave extract, unreacted zinc and corrosion product and also to detect the carbon base and inorganic functional groups present (Okewale and Omoruwuo, 2018). The analysis was carried out using Agilent Technology, FT-IR (Cary 630) Fourier Transform Infrared Spectrophotometer, by scanning the sample through full scale wave number range (4000-650 cm^{-1}).

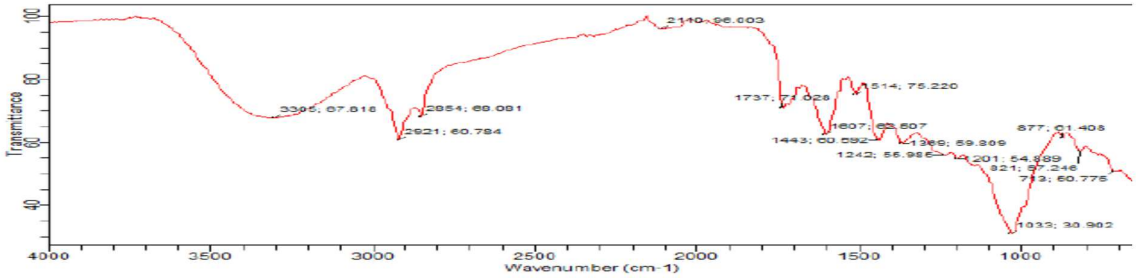

Figure 9(a): FT-IR Spectrum of the neem leave extract

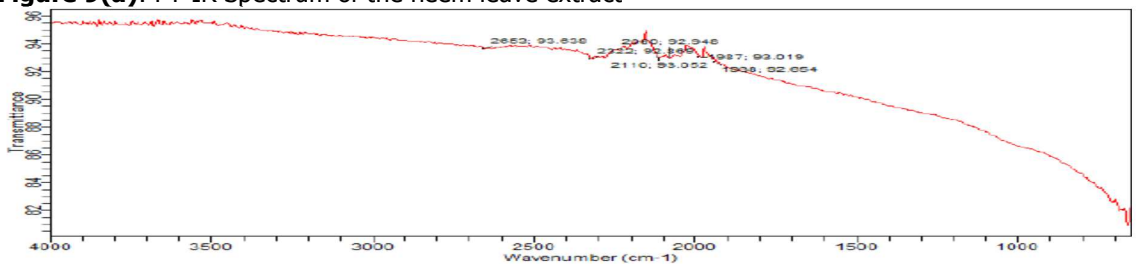

Figure 9(b): FT-IR Spectrum for the unreacted zinc sample

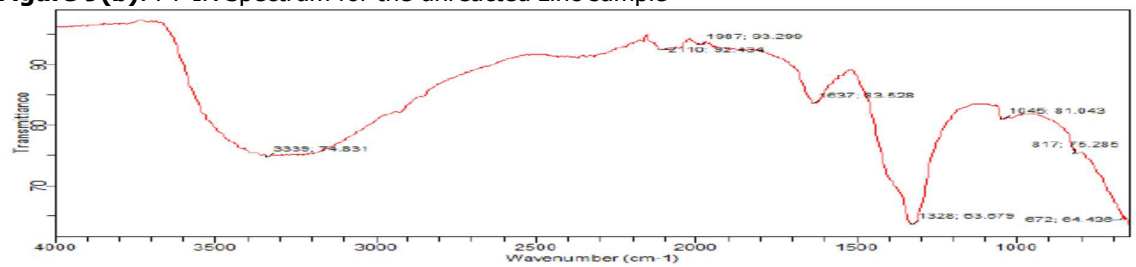

Figure 9(c): FT-IR Spectrum of the inhibited solution by neem leave extract

Recent research shows that compounds that have corrosion inhibition potential contain functional group of hydroxyls (-OH), carboxyl (-COOH), carbonyl (=CO), amine (-C=N) and other functional group that have electron pair (Stiadi *et al.,* 2020). The FT-IR spectrum of neem leave extract is shown in Figure 9 (a). the original absorption band at 3305 cm^{-1} is the wavenumber of –OH (alcohol), and 2100 cm^{-1} is the wavenumber of C=C stretching vibration, absorption band at 1737 cm^{-1} is the wavenumber of C=O (ester). This infrared spectrum indicate the chemical content in neem leave extract that have the potential of inhibition the corrosion of metal in acidic media by formation of stable complex.

Result in Figure 9 (b) show the FT-IR spectrum of unreacted zinc sample and the show no any sharp peak due to the absence of organic content on metal surface. Result in Figure 9 (c) show the FT-IR spectrum layer that was formed on the zinc surface after immersed in 0.5 M HNO_3 with inhibitor. It was observed from this spectrum that –OH stretch at 3305 cm^{-1} shifted to 3339 cm^{-1} and C=O cm^{-1} at 1737 cm^{-1} shifted to 1637 cm^{-1}.

The shift or changes observed in the FT-IR spectrum layers on zinc surface or corrosion product which is different from the spectrum obtained for the ethanolic extract of leave, indicated that the interaction occurred between extract and the zinc surface and suggested physical adsorption. It can be said that the extract has a protective effect due to the presence of the above mentioned functional groups, and therefore can inhibit the corrosion rate of zinc (Srikanth and Sivakumar, 2020; Itodo *et al.,* 2018; Stiadi *et al.,* 2020).

c. Scanning Electron Microscopy (SEM)

Surface examination of zinc specimen was conducted using scanning electron microscopy (SEM) model (PR: X : phenonm World 800-07334), corroded zinc sample, unreacted zinc, and inhibited zinc sample in neem leave extract were analysed and the results are presented in Plate 1, 2, and 3 respectively.

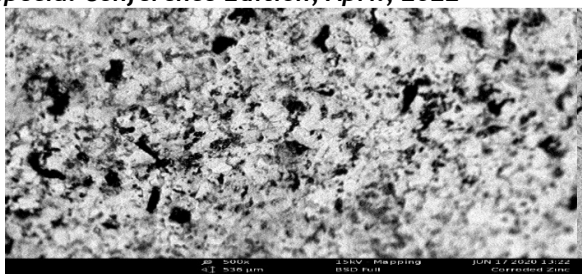

Plate 1: SEM micrograph for uninhibited zinc in HNO_3 solution

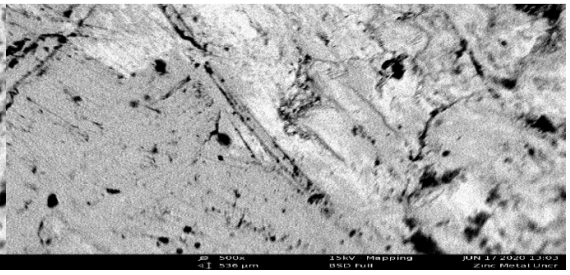

Plate 2: SEM micrograph for unreacted zinc

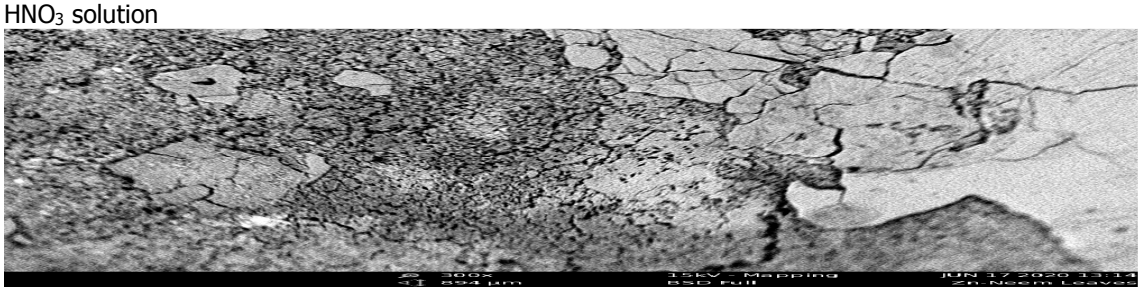

Plate 3: SEM micrograph for inhibited zinc in HNO_3 solution

The results shows that SEM micrograph of zinc in inhibited solution of HNO_3 by neem leave extract has a smooth surface as compare to the rough and crack surface of zinc in uninhibited solution of HNO_3. This is due to the adsorption of the plant extract on the metal surface which reduce the level of corrosion by HNO_3.

d. Adsorption Isotherms

The surface coverage θ value was calculated using equation 4. The surface coverage was used to test five different isotherms which include Langmuir, Freundlich, Temkin, Flory-Huggins and Frumkin isotherm. Freundlich adsorption isotherm was found to be the best fit isotherm among them due to high value of correlation coefficient (R^2). The result of the Freundlich isotherm was plot using linear graph of $log\theta$ against $logC$ and the result are presented in Figure 6.

Therefore since the experimental data obey Freundlich adsorption isotherm, the adsorption mechanism can be described as physisorption which implies that the adsorbed species were adsorbed physically on the surface of the metal and it also involved multilayer of adsorbate on the outer surface of the adsorbent (Okafor *et al.,* 2010; Olanrewaju *et al.,* 2019). Also, the value of the Freundlich factor n is less than 1 which implies ease of adsorption of inhibitor molecule on to the metal surface. The Freundlich equations can be expressed as follows:

$$log\theta = logK + \frac{1}{n}logC \qquad (15)$$

The free energy of adsorption, enthalpy and entropy were calculated using the following equations:

$$\Delta G^0_{ads} = -RTln\,(55.5K_{ads}) \qquad (16)$$

$$log\frac{C_R}{T} = \left(log\frac{R}{Nh} + \frac{\Delta S}{2.303R}\right) - \frac{\Delta H}{2.303RT} \qquad (17)$$

Where 55.5 is the concentration of water in the solution in 1 mol.dm^{-3}, R is the universal gas constant and T is the thermodynamic temperature, ΔG^0_{ads} is the standard free energy (kJ.mol^{-1}). Equation (17) is called transition state equation, where C_R is the corrosion rate, h is the Plank's constant (6.626176×10^{-34} Js), N is the Avogadro's number (6.02252×10^{23} mol^{-1}), R is universal gas constant. The plot of log C_R/T versus 1/T gives a straight line with slope of [-ΔH/2.303R] and intercept of [log R/Nh + ΔS/2.303R] from which the values of ΔH and ΔS were calculated.

The activation energy was calculated using Arrhenius equation:

$$\ln C_R = \ln A - \frac{E_a}{RT} \qquad (18)$$

The plot of ln C_R against 1/T gives a straight line with slope of $-E_a$ / R from which the activation energies was calculated (Abeng *et al.,* 2017).

e. Thermodynamic and Kinetic Studies

The results of change in Gibbs free energy ΔG, K_{ads} value, correlation coefficient at various temperature are presented in the Table 3.

Table 3: Change in Gibbs Free-Energy, K_{ads} values and Correlation coefficient at various Temperature.

ΔG (kJmol^{-1})				K_{ads}				R^2			
303K	313K	323K	333K	303K	313K	323K	333K	303K	313K	323K	333K
-5.75	-7.75	-8.62	-9.48	0.1771	0.3543	0.4468	0.5542	0.9992	0.9968	0.9985	0.9989

The results show that increase in temperature increases the negative value of free energy of adsorption. The negative values of free energy obtained implies that adsorption process was spontaneous and there was a stability of the adsorbed inhibitor layer on the metal surface. Hence, the values of the standard free energy of adsorption obtained are less than -20 kJmol^{-1} coupled with the decreased in the inhibition efficiencies with rise in temperature suggested physical adsorption or physisorption mechanism prevails, otherwise if the values are more negative than -40 kJmol^{-1} indicate chemical adsorption or chemisorption mechanism (Nnanna *et al.,* 2012; Loto *et al.,* 2015; Abakedi and Asuquo, 2016).

Enthalpy ΔH_{ads} and entropy ΔS_{ads} change of the corrosion process were calculated at various inhibitor concentrations, and the results were presented in Table 4. The values of activation enthalpy from the result are all positive in the absence and presence of inhibitor and the values of inhibited are higher than that of uninhibited. The positive sign is an indication of the endothermic nature of the Zinc dissolution process (El hajjaji *et al.,* 2011).

Also the values of ΔH_{ads} were found to increase in the presence of inhibitors, which suggest an increase in the energy barrier of the corrosion reaction, hence the dissolution of zinc metal becomes difficult (Itodo *et al.,* 2018). On the other hand, the values of entropy are all negative which indicates that activated complex in the rate-determining step represent association rather than dissociation, that is there are decrease in the disorderliness from the reactant to activated complex taking place (Noor, 2007; Khadraoui *et al.,* 2013).

Table 4: Activation energy, Enthalpy and Entropy of adsorption at different inhibitor concentration

Inhibitor Con. (g/L)	Activation energy (E_a) kJmol^{-1}	Enthalpy (ΔH_{ads}) kJmol^{-1}	Entropy (ΔS_{ads}) Jmol^{-1}
0.00	11.89	9.25	-0.1086
0.20	14.81	12.17	-0.1003
0.40	17.49	14.85	-0.0927
0.60	21.28	18.64	-0.0818
0.80	26.80	24.16	-0.0655

The activation energy result was presented in Table 4. The result show that addition of neem leave extract up to 0.80 g/L in 0.5 M HNO_3 solution increases the activation energy. This can be attributed to the fact that higher value of E_a in the presence of inhibitor compared to its absence are generally consistent with a physisorption, while unchanged or lower value of E_a in inhibited solution suggest charge sharing or transfer from the organic inhibitor to the metal surface to form coordinate covalent bond (Noor and Al-Moubaraki, 2008; Nahle *et al.,* 2012).

Computational studies

a. Frontier molecular orbital

The effectiveness of inhibitor molecules in reducing the level of acid corrosion can not only be restricted on molecular structure, but also on molecular orbitals electronic distribution. Among quantum chemical methods for evaluation of corrosion inhibitors, density functional theory (DFT) has proven to be the powerful method of calculating the ground state molecular properties of a molecule, which shown significant promise and appear to be adequate for pointing out the changes in electronic structure responsible for inhibition action (Udhayakala *et al.,* 2012; Obi-Egbedi and Ojo, 2015).

The frontier molecular orbitals HOMO and LUMO help to characterize the chemical activity and kinetic stability of the molecule. The region of high (HOMO) density measures the electron donating ability of the molecule to the metal surface while the LUMO region measures the capability of the molecule to accept electrons from the d-orbital of the metal by back bonding (Seda *et al.,* 2014; Umaru and Ayuba, 2020a).

The region of HOMO in the studied molecules as shown in the Figure 10(c) – 12(c) are usually saturated on carbonyl functional (-C=O), chloride and aromatic carbon atom (-C=C-) of the inhibitor, while the (LUMO) orbitals are presented in the Figure 10(d) – 12(d) that has the ability to accept free electrons in the p-orbital of the metal using antibonding orbitals to form back bonding (Al-Mazaideh *et al.,* 2016). Figure 10, 11 & 12 depict the structures of geometry optimized, electron density, HOMO and LUMO orbital of the

molecules. It can be observed that the HOMO orbitals are distributed along carbonyl carbon and conjugated carbon on benzene ring. This can be attributed to the region of high electron transfer in the molecule (Seda *et al.,* 2014).

The LUMO orbitals are distributed across the adjacent carbon containing the heteroatom. This implies the region of less electronegativity in the molecules (Ayuba *et al.,* 2020). The optimized electronic structure of the molecule conform to the structure with energy minima with no imaginary frequencies (Umaru and Ayuba, 2020a). From the optimized structure of the molecules, it is observed that the molecules are almost planar in shape which provides a better orientation for strong adsorption onto the metal surface.

The overlap of the total electron density all around each molecule also facilitates the flat orientation of the molecules on the zinc metal surface. Figures 10, 11, & 12 show the electronic and structural properties of the three studied molecules as follows: a) Geometry Optimized Molecule b) Total Electron Density c) Highest Occupied Molecular Orbital (HOMO) d) Lowest Unoccupied Molecular Orbital (LUMO).

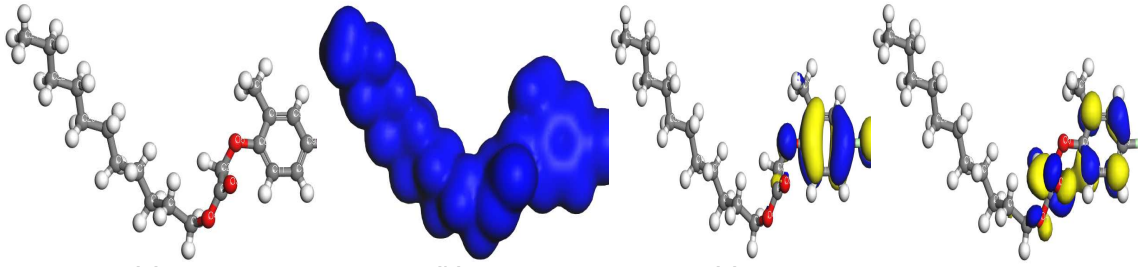

Figure 10: Electronic and structural properties of AME

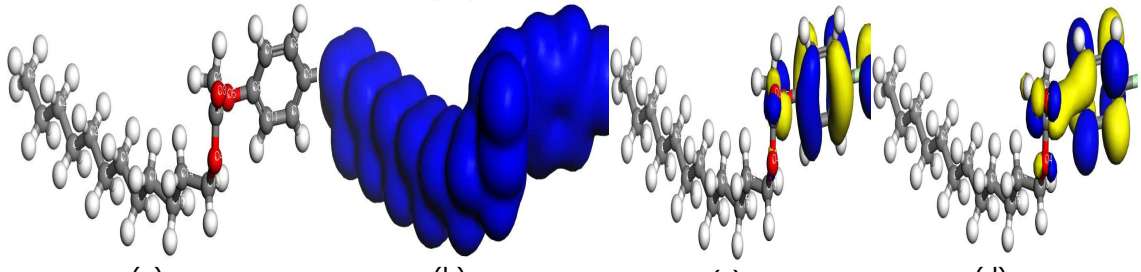

Figure 11: Electronic and structural properties of ADE

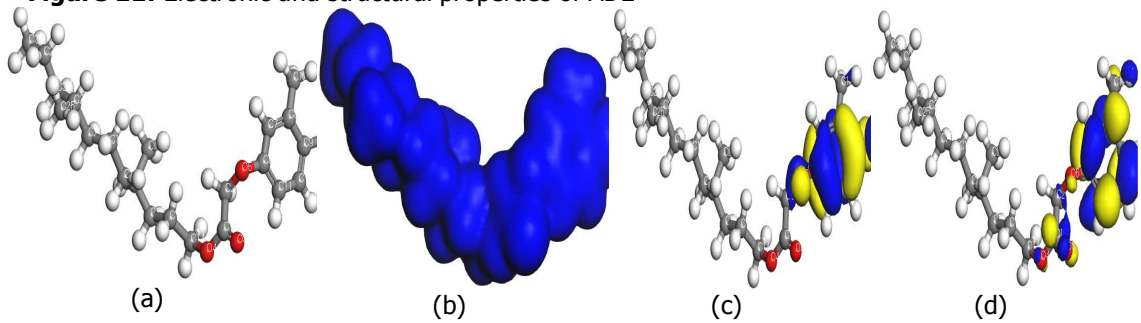

Figure 12: Electronic and structural properties of ADME

b. Frontier Orbital Energy Descriptors

Quantum chemical parameters calculated from Density Functional Theory (DFT) are presented in Table 5. E_{HOMO} represent the energy of the highest occupied molecular orbital and indicated the ability of a molecule to donate electrons to the suitable acceptor molecule of low empty molecular orbital energy (E_{LUMO}), while E_{LUMO} represents the energy of lowest unoccupied molecular orbital and shows the ability to accept electrons. Hence, the binding ability of the inhibitor to the metal surface increases when increasing E_{HOMO} and decreasing E_{LUMO} (Hammouti *et al.,* 2010; Al-Mazaideh *et al.,* 2016).

Therefore, with regard to the E_{HOMO} values of the studied molecules, the inhibition efficiency follow the trend: AME>ADE>ADME while interms of ELUMO the inhibition efficiency of the inhibitor molecules follows the order: ADE>ADME>AME. In terms of energy gap ΔE the inhibition action of

the molecules follow: AME>ADE>ADME, this can be attributed to the fact that low values of ΔE increases the reactivity of the molecule and improved inhibition efficiencies of organic inhibitor, because the energy needed to remove an electron from the highest occupied orbital will be minimized (Benedetti *et al.,* 2015; El Hendawy *et al.,* 2021).

Chemical hardness (η) is the resistance against electron cloud polarization. Therefore as the hardness (η) value of the molecule increases, its inhibition efficiency decreases since hard molecules resist electron donation. In contrary to the above statement, soft molecules are good corrosion inhibitors, the greater the softness, the higher the inhibition efficiency (Ogunyemi and Adejoro, 2019; Ayuba and Umar, 2021). The result of the Global hardness and softness are presented in Table 5 and the trend in inhibition efficiency of the studied molecule with respect to hardness and softness are: ADE=AME>ADME.

The fraction of electrons transferred from inhibitor molecules to the metal surface was calculated from equation (13). According to report by (Ayuba and Umar, 2021) states that if $0 < \Delta N > 3.6$, the inhibitor molecule has strong tendency to donate electrons to the empty orbitals of the metal. Therefore, the molecules follow the trend AME>ADME>ADE in terms ΔN, and the result indicated that all molecules can donate electrons to the vacant orbitals of zinc to formed coordinate bonds. The energy of back donation (ΔE_{b-d}) is the amount of energy change when an inhibitor molecule receives and back-donates certain amount of charge (Udhayakala *et al.,* 2012). In terms of (ΔE_{b-d}), the most favourable situation corresponds to the case when the total energy change (ΔE_{b-d}) is minimum.

Hence, the molecules follow the trend AME>ADE>ADME. In general, molecule AME and ADE has similar and better values of frontier orbital energy compared to ADME which make them to have better protection toward acid corrosion of zinc due to similar structure and number of carbon atom, while it was observed that increase in the number substituent in ADME decrease the protection ability of the molecule.

Table 5: Calculated quantum chemical parameters for the studied molecules

Parameters	**Inhibitor molecules**		
	AME	**ADE**	**ADME**
HOMO (at orbital number)	96	96	104
LUMO (at orbital number)	97	97	105
E_{HOMO}	-5.974	-6.305	-6.258
E_{LUMO}	-0.249	-0.579	-0.287
Energy gap (ΔE) (eV)	5.725	5.726	5.971
Molecular weight ($gmol^{-1}$)	200.6	354.9	382.5
Ionization potential (I) (eV)	5.974	6.305	6.258
Electron Affinity (A) (eV)	0.249	0.579	0.287
Global hardness (η)	2.863	2.863	2.9855
Global softness (σ)	0.3493	0.3493	0.3350
Absolute Electronegativity (χ)	3.1115	3.442	3.2725
Fraction of Electron Transfer (ΔN)	0.3221	0.2427	0.3012
Energy of back-donation (ΔE_{b-d})	-0.7156	-0.7158	-0.7464

c. Molecular Dynamic Simulation

The results of adsorption parameters for the interaction of the studied molecules with the Zn (1 1 0) surface were calculated via forcite quench dynamics and presented in Table 6. The equilibrium adsorption configuration of the three molecules are shown in Figure (13-15). Result in Table 6 show that ADE inhibitor molecule has the highest adsorption energy among the molecules, with ADME having the least adsorption energy. This is because ADE has a flat lying interaction with the zinc (1 1 0) surface that facilitate in strong interaction between the molecule and metal surface as shown in the Figure 14(a & b) for side view and top view snap shot respectively. This orientation results to disposition of large surface area on the Zn (1 1 0) surface for interaction with the molecules and consequently, higher inhibition efficiency is observed due to higher negative value of binding energy (Umaru and Ayuba, 2020a). AME also has a better interaction with the metal surface when compared with ADME which result in having higher adsorption energy than the later.

Therefore, the inhibition efficiency observed in experimental analyses could be due to the strong interaction between ADE inhibitor molecule and zinc (1 1 0) surface, which provide protection to the metal surface. It was also reported by (Ayuba *et al.,* 2020; Umaru and Ayuba, 2020a) that adsorption energy greater than 100 kcal/mol or binding energy greater than -100 kcal/mol are associated with chemical adsorption, while values lower than that signifies physical adsorption.

Table 6: Adsorption parameters for the interaction of the studied molecules with Zn (1 1 0) surface

Parameters	**Inhibitor molecules**		
	AME	**ADE**	**ADME**
Total Kinetic Energy (kcal/mol)	34.18 ± 2.24	41.77 ± 1.13	33.28 ± 2.14
Total Potential Energy (kcal/mol)	-29.26 ± 0.84	-57.38 ± 1.85	-22.54 ± 0.17
Energy of Molecule (kcal/mol)	-17.94 ± 0.48	-18.09 ± 0.04	-12.51 ± 0.33
Energy of Zn (1 1 0) Surface (kcal/mol)	0.00 ± 0.00	0.00 ± 0.00	0.00 ± 0.00
Binding Energy (kcal/mol)	-11.32	-39.29	-10.02
Adsorption Energy (kcal/mol)	11.32 ± 1.14	39.29 ± 1.87	10.02 ± 0.16

The equilibrium adsorption configuration of the molecule are shown in the Figures 13, 14 and 15.

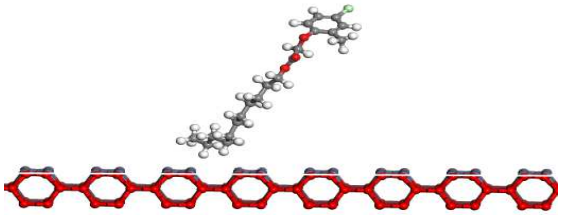

Figure 13a: Side view of AME

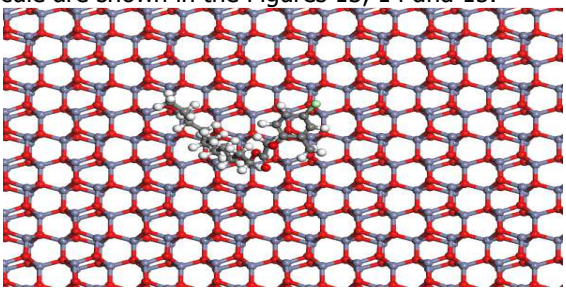

Figure 13b: Top view of AME

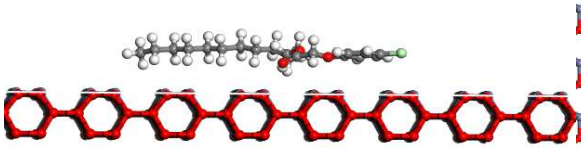

Figure 14a: Side view of ADE

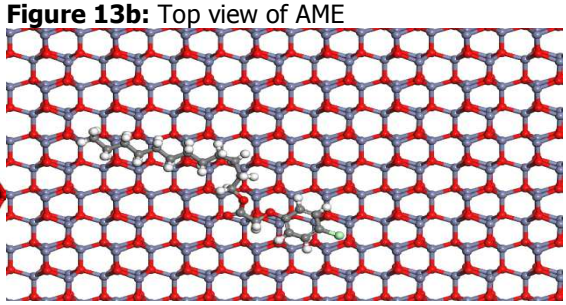

Figure 14b: Top view of ADE

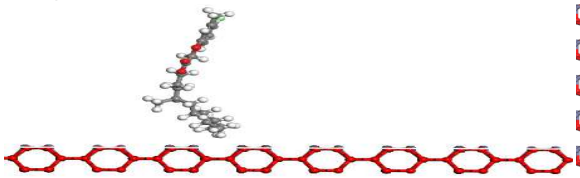

Figure 15a: Side view of ADME

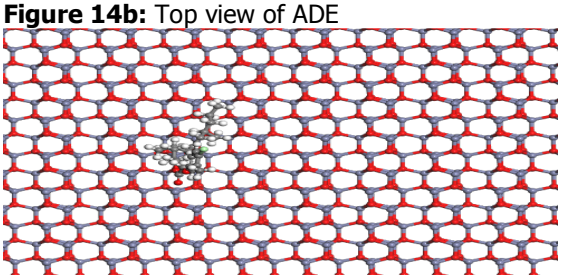

Figure 15b: Top view of ADME

CONCLUSION

The neem leave extract show an excellent performance toward reducing the corrosion of zinc in nitric acid. The inhibition efficiency of the extracts was found to increase with increased in inhibitor concentration reaching 53.09% at 4 hours immersion time. Adsorption isotherm studies show that the mechanism of adsorption of inhibitor molecule on to the metal surface follow Freundlich isotherm suggesting physical adsorption. Computation studies reveal that ADE has high adsorption energy compared to AME and ADME due to the strong interact with Zn (1 1 0) surface as such it has high inhibition efficiency. The observed experimental inhibition efficiency can be correlate to the adsorption of such molecules of inhibitor on to the metal surface by providing protection against nitric acid attack toward zinc metal.

REFERENCES

Abakedi, O. U. and Asuquo, J. E. (2016). Corrosion Inhibition of Aluminium in Acidic Medium by Ethanol Leaf Extract of *Azadirachta indica*. *J. basic appl. Res.* 2(4): 556-560.

Abeng, F. E. Idim, V. D. and Nna, P. J. (2017). Kinetics and Thermodynamic Studies of Corrosion Inhibition of Mild Steel Using

Methanolic Extract of *Erigeron floribundus* (Kunth) in 2 M HCl Solution. *J. World News of Natural Sciences*. 10: 26-38.

Al-Mazaideh, G. M. Al-Zereini, W. A. Al-Mustapha, A. H. and Khalil, S. M. (2016). The effect of nitro maleimides from a marine vibrio species compounds as a new source of environmentally friendly corrosion inhibitors for metals. *Advances in Environmental Biology*, 10(8): 159-168.

Al-Saadi, K. A. and Al-Safi, S. A-J. (2011). Potentiostatic Study for the effect of LAS on the Corrosion of pure Zinc in 0.01 M HCl Solutions. *Ibn al-haitham j. for pure & appl. Sci.*, 24(2): 1-16.

Ayuba, A. M. and Umar, U. (2021). Modeling Vitexin and Isovitexin Flavones as Corrosion Inhibitors for Aluminium Metal. *Karbala International Journal of Modern Science,* 7(3): 1-12.

Ayuba, A. M. Thomas, A. N. and Abdulfatah, S. M. (2020). Density functional theory and molecular dynamic simulation studies on the corrosion inhibition of some thiosemicarbazide derivatives on aluminium metal. *Journal of Applied Surfaces and Interfaces*, 8: 7-14.

Ayuba, A. M. Uzairu, A. Abba, H. and Shallangwa, G. A. (2018). Theoretical study of aspartic and glutamic acids as corrosion inhibitors on aluminium metal surface. *Mor. J. Chem.*, 6(1): 160-172.

Benedetti, A. V. Teixeira, D. A. Valente Jr, M. A. G. Feliciano, G. T. da Silva, S. C. and Fugivara, C. S. (2015). Experimental and Theoretical Studies of Volatile Corrosion Inhibitors Adsorption on Zinc Electrode. *J. Braz. Chem. Soc.,* 26(3): 434-450.

Dalhatu, A. A. Sani A. I. Sani B. S. and Sani D. N. (2018). Study of the Inhibitive Property of *Azadirachta indica* (Neem Tree) Gum on Mild Steel Corrosion in Various Acidic Media. *International Research Journal of Pure & Applied Chemistry.* 17(3): 1-11.

Dubey, R. S. (2020). Green Corrosion Inhibitos for Metals and Alloys: A Comprehensive Review. *International Journal of Advance Research*. 8(6): 1558-1565.

El hajjaji, S. Najoua, L. Fouad, B. Mounim, L. and Charafeddine, J. (2011). Study of Temperature Effect on the Corrosion Inhibition of C38 Carbon Steel Using Amino-tris(Methylenephosphonic) Acid in Hydrochloric Acid Solution. *Hindawi Publishing Corporation International Journal of Corrosion*. 548528. Doi:10.1155/2011/548528

El Hendawy, M. M. Kamel, A. M. Mohammed, M. M. A. Boukherroub, R. Ryl, J. and Amin, M. A. (2021). Diaryl Sulfide Derivatives as Potential Iron Corrosion Inhibitors: A Computational Study. *Molecules,* 26, 6312.

Elmsellem, H. Lahmidi, S. Sebbar, N. K. El Ouasif, L. Jilalat, A. E. Elyoussfi, A. Dafali, A. Hammouti, B. El Mahi, B. Essassi, E. M. and Abdel-Rahman, I. (2017). Corrosion inhibition of mild steel by two new 1,2,4-triazolo[1,5-a] pyrimidine derivatives in 1 M HCl: Experimental and computational study. *Journal of materials and Environmental Sciences*. 8(1): 225-237.

Hammouti, B. Mihit, M. Laarej, K. El Makarim, H. A. Bazzi, L. and Salghi, R. (2010). Study of the inhibition of the corrosion of copper and zinc in HNO_3 solution by electrochemical technique and quantum chemical calculations. *Arabian Journal of Chemistry*. 3: 55-60.

Itodo, A. U. Aondofa B. G. and Iorungwa M. S. (2018). Retarding Mild Steel Corrosion using a Blend of Schiff Base Metal Complex and Neem Plant Extract. *ChemSearch Journal* 9(2): 45 – 63.

Jane, N. M. and Nakara, M. T. (2019). Determination of the Corrosion Inhibition Effect of *Terminalia Ivorensis* Leave Extract on Galvanized and Mild Steel in Sulphuric Acid Media. *American Journal of Physical Chemistry*. 8(1): 11-16.

Khadraoui, A. Khelifa, A. Hamitouche, H. and Mehdaoui, R. (2013). Inhibitive effect by extract of *Mentha rotundifolia* leave on the corrosion of steel in 1 M HCl solution. *Res. Chem. Intermed*. Doi: 10.1007/s11164-012-1014-y

Loto C. A. Joseph, O. O. Loto, R. T. and Okeniyi, J. O. (2015). Adsorption and Inhibitive Properties of *Camellia Sinensis* for mild steel in 0.5M HCl and 0.8M H_2SO_4. *NACE Internation; Corrosion 2015 Conference & Expo*. Paper no: 5655.

Madkour, L. H. and Elshamy, I. H. (2016). Experimental and Computation Studies on the Inhibition performances of benzimidazole and its derivatives for the corrosion of copper in nitric acid. *Int. J. Ind. Chem.*, 7: 195-221.

Nahle, A. Abu-Abdoun, I. I. and Abdel-Rahman, I. (2012). Inhibition of Mild Steel Corrosion by 3-benzoylmethyl benzimidazolium hexafluoro antimonite in Acidic Solution. *Hindawi Publishing Corporation International Journal of Corrosion*. doi:10.1155/2012/246013

Nnanna, L. A. Obasi, V. U. Nwadiuko, O. C. Mejeh, K. I. Ekekwe, N. D. and Udensi, S. C. (2012). Inhibition by *Newbouldia leavis* Leaf Extract of the Corrosion of Aluminium

in HCl and H_2SO_4 Solutions. *Archives of Applied Science Research*. 4(1): 207-217.

Noor, E. A. (2007). Temperature Effects on the Corrosion Inhibition of Mild Steel in Acidic Solutions by Aqueous Extract of Fenugreek Leave. *Int. J. Electrochem. Sci.*, 2: 996-1017.

Noor, E. A. and Al-Moubaraki, A. H. (2008). Thermodynamic study of metal corrosion and inhibitor adsorption processes in mild steel/1-methyl-4[4'(-X)-styryl pyridinium iodides/hydrochloric acid systems. *Material Chemistry and Physics*. 110: 145-154.

Obi-Egbedi, N. O. and Ojo, N. D. (2015). Computational studies of the corrosion inhibition potentials of some derivatives of 1H-Imidazo [4, 5-F] [1, 10] phenanthroline. *Journal of Science Research*, 14**:** 50-56.

Ogunyemi, B. T. and Adejoro, I. A. (2019). Corrosion Inhibition Potential of Four Phenyltetrazoles Derivatives using Density Functional Theory and Quantitative Structure-Activity Relationship Approach. *J. Appl. Sci. Environ. Manage.*, 23(4): 665-671.

Okafor P. C. Ebenso E. E. and Ekpe U. J. (2010). *Azadirachta indica* Extracts as Corrosion Inhibitor for Mild Steel in Acid Medium. *Int. J. Electrochem. Sci.*, 5: 978 – 993.

Okewale, A. and Omoruwuo, F. (2018). Neem Leaf Extract as a Corrosion Inhibitor on Mild Steel in Acidic Solution. *International Journal of Engineering Research in Africa*. 35: 208-220.

Olanrewaju, A. Oluseyi, A. K. Ayomide, B. V. Theresa, A. O. and Oluwakayode, A. S. (2019). Corrosion inhibitive properties of *Epimedium grandiflorum* on mild steel in HCl acidic media. *IOP Conf. Series: Materials Science and Engineering*. 509: 012008.

Seda, S. Yesin, K. and Filiz, K. (2014). Theoretical Study of 11-thiocyanatoundecanoic acid phenylamide derivatives on corrosion inhibition efficiencies. *Can. J. Chem.*, 92: 876-887.

Seifzadeh, D. Ashassi-Sorkhabi, H. and Hosseini, M. G. (2008). EN, EIS and polarization studies to evaluate the inhibition effect of 3H-phenothiazin-3-one, 7-dimethylamin on mild steel corrosion in 1 M HCl solution. *J. Corrosion Science*. 50: 3363-3370.

Sharma S. K. Peter A. and Obot I. B. (2015). Potential of *Azadirachta indica* as a green corrosion inhibitor against mild steel, aluminum, and tin: a review. *Journal of Analytical Science and Technology*. 6(26): DOI 10.1186/s40543-015-0067-0.

Sharma, S. K. and Peter, A. (2017). Use of *Azadirachta indica* (AZI) as green corrosion inhibitor against mild steel in acidic medium: anti-corrosive efficacy and adsorptive behaviour. *Int. J. Corros. Scale Inhib.*, 6(2): 112-131.

Sobhi, M. El-Noamany, H. H. and El-Etre, A. Y. (2015). Inhibition of Carbon Steel corrosion in Acid medium by *Eruca sativa* Extract. *Journal of Basic and Environmental Sciences*. 2: 9-18.

Srikanth, A. P. and Sivakumar, P. R. (2020). Green corrosion inhibitor: A comparative study. *Sadhana indian Academy of Science*. https://doi.org/10.1007/s12046-020-1283-x

Stiadi, Y. Rahmayeni, Rahmawati, L. Efdi, M. Aziz, H. and Emriadi, (2020). "*Mangifera odorata* Griff Seed Extract as Corrosion Inhibitor of Mild Steel in Hydrochloric Acid Medium". *Rasayan Journal of Chemistry*. 13(1): 230-239.

Tuaweri, T. J. Ogbonnaya, E. A. Onyemaobi, O. O. (2015). Corrosion Inhibition of Heat Treated Mild Steel with Neem Leave Extract in a Chloride Medium. *International Journal of Research in Engineering and Technology*. 4(6): 404-409.

Udhayakala, P. Rajendiran, T. V. and Gunasekaran, S. (2012). Density Functional Theory Investigations for the adsorption of some Oxadiazole Derivatives on Mild Steel. *Journal of Advanced Scientific Research*, 3(3): 67-74.

Umaru, M. and Ayuba, A. M. (2020). Computational studies of Anticorrosive Effect of Some Thiazole Derivatives against the Corrosion of Aluminium. *Rhazes Academic Scienctific Journals*, 10: 113-128.

Umaru, M. and Ayuba, A. M. (2020). Quantum chemical calculations and molecular dynamic simulation studies on the corrosion inhibition of aluminium metal by myricetin derivatives. *Journal of New Technology and Materials*, 10(02): 18-28.

Vashi R. T. and Patel K. K. (2015). *Azadirachta indica* Extract as corrosion Inhibitor for Copper in Nitric Acid Medium. Research *Journal of Chemical Sciences*. 5(11): 59-66.

Venkata N. T. and Pankaj G. (2017). Corrosion inhibition and adsorption properties of *Azadirachta indica* (Neem) leave extract as a green inhibitor for Zinc in H_2SO_4. *International Journal of Current Research*. 9(12): 63131-63135.